ResearchGate

See discussions, stats, and author profiles for this publication at: https://www.researchgate.net/publication/11766648

Effect of the Central Disulfide Bond on the Unfolding Behavior of Elongation Factor Ts Homodimer from Thermus thermophilus †

ARTICLE *in* BIOCHEMISTRY · SEPTEMBER 2001

Impact Factor: 3.02 · DOI: 10.1021/bi010274e · Source: PubMed

CITATIONS
12

READS
10

5 AUTHORS, INCLUDING:

Erik Sedlák
Pavol Jozef Šafárik University in Košice
53 PUBLICATIONS **905** CITATIONS
SEE PROFILE

Marian Antalik
Pavol Jozef Šafárik University in Košice
118 PUBLICATIONS **977** CITATIONS
SEE PROFILE

Mathias Sprinzl
University of Bayreuth
274 PUBLICATIONS **9,836** CITATIONS
SEE PROFILE

Available from: Erik Sedlák
Retrieved on: 24 January 2016

Effect of the Central Disulfide Bond on the Unfolding Behavior of Elongation Factor Ts Homodimer from *Thermus thermophilus*†

Erik Sedlák,‡ Eva Valušová,‡ Martina Nesper-Brock,§ Marián Antalík,‡,|| and Mathias Sprinzl*,§

Department of Biochemistry, Faculty of Science P. J. Šafárik University, Košice, Slovakia, Department of Biophysics, Institute of Experimental Physics, Slovak Academy of Sciences, Košice, Slovakia, and Laboratorium für Biochemie, Universität Bayreuth, D-95440 Bayreuth, Germany

Received February 7, 2001; Revised Manuscript Received May 30, 2001

ABSTRACT: Functionally active elongation factor Ts (EF-Ts) from *Thermus thermophilus* forms a homodimer. The dimerization interface of EF-Ts is composed of two antiparallel β-sheets that can be connected by an intermolecular disulfide bond. The stability of EF-Ts from *T. thermophilus* in the presence and absence of the intermolecular disulfide bond was studied by differential scanning calorimetry and circular dichroism. The ratio of the van't Hoff and calorimetric enthalpies, $\Delta H_{vH}/\Delta H_{cal}$, indicates that EF-Ts undergoes thermal unfolding as a dimer independently of the presence or absence of the disulfide bond. This can be concluded from (1) the presence of residual secondary structure above the thermal transition temperature, (2) the absence of concentration dependence, which would be expected for dissociation of the dimer prior to unfolding of the monomers, and (3) a relatively low heat capacity change (ΔC_p) upon unfolding. The retained dimeric structure of the thermally denatured state allowed for the determination of the effect of the intermolecular disulfide bond on the conformational stability of EF-Ts, which is $\Delta\Delta G_{(S-S,SH\ HS)} = 10.5$ kJ/mol per monomer at 72.5 °C. The possible physiological implications of the dimeric EF-Ts structure and of the intersubunit disulfide bond for the extreme conformational stability of proteins in thermophiles are discussed.

The bacterial elongation factor Ts (EF-Ts)[1] acts as a nucleotide exchange factor in the functional cycle of elongation factor Tu (EF-Tu) and accelerates the guanine nucleotide release from EF-Tu·GDP. While EF-Ts from *E. coli* (*1*) is monomeric, its homologue in *T. thermophilus* is active as a dimer (*2*−*4*). The crystal structures of EF-Ts in complex with EF-Tu from both mesophilic (*E. coli*) (*1*) and thermophilic (*T. thermophilus*) (*2*) organisms revealed that despite substantial differences in the length of the polypeptide sequence and the quaternary structure, the *E. coli* EF-Ts monomer structurally mimics the *T. thermophilus* EF-Ts dimer. The arrangement of secondary structure elements in *E. coli* EF-Ts including the biparite interface is very similar to that of the *T. thermophilus* EF-Ts dimer, $(EF\text{-}Ts)_2$. Both the symmetrical dimerization domain of *T. thermophilus* EF-Ts (Figure 1) and the pseudo-symmetrical bipartite interface of *E. coli* EF-Ts (*1*) are stabilized mainly by van der Waals contacts between hydrophobic residues located in three antiparallel β-strands. While the *E. coli* EF-Ts bipartite interface is covalently connected by a peptide bond, the *T.*

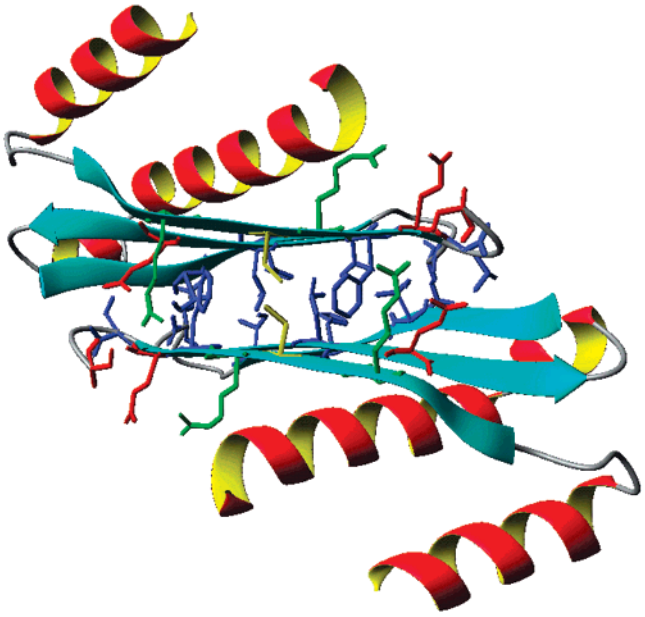

FIGURE 1: Dimerization interface of *Thermus thermophilus* EF-Ts. The interface is stabilized by an intermonomer disulfide bridge (yellow), hydrophobic interactions (blue), and ionic interactions (negatively charged amino acids, red; positively charged amino acids, green). Several intramonomer hydrophobic interactions also occur between the three-stranded β-sheet and the closest helix 5 (not shown for clarity).

† Supported by the Deutsche Forschungsgemeinschaft (Sp 243/8-2), Bundesministerium für Bildung und Forschung (BMBF, SVK 98/002), Fonds der Chemischen Industrie, Slovak Ministry of Education, and Slovak Grant Agency (Grant 7023). Dedicated to the memory of the late P. B. Sigler.

* Correspondence should be addressed to this author at the Laboratorium für Biochemie, Universität Bayreuth, D-95440 Bayreuth, Germany. Fax: +49 921 552432. E-mail: mathias.sprinzl@uni-bayreuth.de.

‡ Faculty of Science P. J. Šafárik University.

§ Universität Bayreuth.

|| Slovak Academy of Sciences.

[1] Abbreviations: EF-Ts, elongation factor Ts; EF-Ts(wt), EF-Ts wild type; EF-Ts(C190A), EF-Ts with cysteine 190 replaced with alanine; EF-Tu, elongation factor Tu; DSC, differential scanning calorimetry; CD, circular dichroism; ASA, accessible surface area.

10.1021/bi010274e CCC: $20.00 © 2001 American Chemical Society
Published on Web 07/20/2001

thermophilus EF-Ts monomers may be connected by an intersubunit disulfide bond. The importance of the hydrophobic interaction in EF-Ts from *T. thermophilus* for its function and stability was demonstrated by site-directed mutagenesis (*3*, *4*). The interference with EF-Ts dimerization inhibits binding to EF-Tu and significantly reduces the stability of EF-Ts (*4*). Although noncovalent intermonomer interactions sufficiently stabilize the *T. thermophilus* EF-Ts dimer at the high physiological temperatures, additional stabilization might arise from a disulfide bridge between cysteines 190 of both monomers (*3*, *5*). Interestingly, among all known EF-Ts sequences (*3*, *6*) Cys190 is unique for thermophilic *T. thermophilus* EF-Ts. This is surprising since it is known that cystine residues can undergo heat-induced β-elimination at elevated temperatures (*7*). In accordance with that, there is a preference for hydrophobic residues that replace cysteines in proteins from thermophilic organisms (*8*). Moreover, cysteines are usually expelled from the interface of dimeric proteins (*9*).

Recently, intra- and intermolecular disulfide bridges were identified in several intracellular proteins from thermophilic organisms (*10*−*14*). It is not clear, however, whether the disulfide bonds can form and thus contribute to protein stability in the presumably reducing environment of the bacterial cytoplasm. Although there is no direct evidence for the existence of the disulfide bond in *T. thermophilus* EF-Ts in vivo (*5*), the possibility to induce a covalent linkage in native EF-Ts offers a unique opportunity to study its effect on the stability of the dimer. This is advantageous compared to engineered disulfide bonds where unexpected alterations of the native structure due to amino acid replacements may occur (*15*). The effect of disulfide bridges on protein stability has usually been investigated by intramolecular cross-linking of cysteine residues. Most of these studies suggested that disulfide linkages confer stability primarily by limiting the conformational entropy of the unfolded state (*16*, *17*). In contrast, it was also suggested that disulfide bonds actually destabilize the native state entropically by reducing the exposure of hydrophobic residues to the solvent in the denatured state. In this case, the role of cystine bridges in stabilizing proteins is predominantly enthalpic as a consequence of less favorable hydrogen bonding networks in the cross-linked denatured state relative to those in the absence of disulfide bonds (*18*). Proteins in thermophilic organisms are frequently stabilized by noncovalent assemblies of identical monomeric subunits (*19*−*22*). This observation led to an increased interest in the stabilization effects of covalent intersubunit bonds created either by engineered disulfide bonds (*23*−*26*) or by chemically induced covalent cross-links between protein monomers (*27*).

Dimers of elongation factor Ts from *T. thermophilus* that naturally possess cysteine residues on the subunit interface which are capable of forming a disulfide bond provide a unique opportunity to test the contribution of this covalent linkage to the stability of the dimer. The thermal denaturation of the dimeric elongation factor Ts from *T. thermophilus* was therefore studied in the presence and in the absence of a disulfide bridge by differential scanning calorimetry (DSC). Microcalorimetry is especially suitable to study the thermodynamic parameters of proteins whose melting temperatures are above 100 °C. In this work, we demonstrate that a significant stabilization of *T. thermophilus* EF-Ts homodimer is achieved by an intermonomer disulfide bond.

EXPERIMENTAL PROCEDURES

Analytical-grade biochemicals were obtained from Merck (Germany). Ultrapure guanidine hydrochloride and sodium perchlorate were purchased from ICN, Biomedicals, Inc. Guanidine and urea concentrations were determined from refractive index measurements using an Abbe Refractometer AR3-AR6. Construction, overexpression, and purification of EF-Ts and its variants were done as described by Jiang et al. (*3*). Heat-induced equilibrium unfolding transitions measured by circular dichroism were recorded in a Jasco J-600 spectropolarimeter equipped with a PTC-348 WI Peltier element. The temperature reading was calibrated with a precision thermometer (Brand, Wertheim, Germany). Protein concentrations were 2.5 μM in 10 mM sodium phosphate buffer pH 7.0, and the desired concentration of guanidine hydrochloride in 5 mm path-length cells. The scan rate was 1 K/min. Transitions were monitored by the increase in CD at 222 nm (1 nm bandwidth) on denaturation. The ellipticity is reported as the mean residue ellipticity and was calibrated with (+)-10 camphorsulfonic acid. Nonlinear least-squares regression (Grafit 3.0, Erithacus Software, Staines, U.K.) was performed assuming a two-state equilibrium. Reversibility of folding was examined by comparing the thermal transition of recooled samples with the transition observed at the first heating.

DSC measurements were carried out on a DASM-4 microcalorimeter. The volume of the measuring cell was 0.4786 cm^3. Samples with 50 mM dithiothreitol were incubated at 40 °C for about 30 min prior to calorimetric measurements. All DSC traces were corrected for a sigmoidal baseline and for the difference in heat capacity between the initial and final states (*28*). The calorimetric enthalpy was derived from the area of the heat absorption peak. As the observed heat effect, transition temperature T_{trs}, and the shape of melting curve do not significantly depend on the heating rate (0.5−2 K/min) and protein concentration (0.25−2.0 mg/mL), a van't Hoff analysis for evaluation of thermodynamic measurements was performed (*29*). The van't Hoff enthalpy was calculated from the same calorimetric curve according to eq 1:

$$\Delta H_{vH} = 4RT_{trs}^{2}C_{p,max}/Q_t \qquad (1)$$

where $C_{p,max}$ is the height of the heat capacity peak at the denaturation temperature, T_{trs}, and Q_t is the peak area in Joules. If the transition is of a two-state type without aggregation of proteins, the ratio $\Delta H_{vH}/\Delta H_{cal}$ equals 1. For a process with intermolecular cooperation, $\Delta H_{vH}/\Delta H_{cal}$ is greater than 1, giving an estimation of the number of molecules included in the cooperative units (*30*).

Proteins concentrations were determined by using calculated extinction coefficients at 280 nm according to Pace et al. (*31*): $\epsilon_{EF-Ts(wt)} = 11\,523\ M^{-1}\cdot cm^{-1}$, $\epsilon_{EF-Ts(C190A)} = 11\,460\ M^{-1}\cdot cm^{-1}$.

Thermodynamic Functions. If the heat capacity change upon protein unfolding is not significantly temperature-dependent, the thermodynamic functions for the unfolding transition of a protein can be calculated from

$$\Delta H(T) = \Delta H(T_{trs}) - \Delta C_p(T_{trs} - T) \quad (2)$$

$$\Delta S(T) = \Delta H(T_{trs})/T_{trs} - \Delta C_p \ln (T_{trs}/T) \quad (3)$$

$$\Delta G(T) = \Delta H(T_{trs})(1 - T/T_{trs}) + \Delta C_p(T - T_{trs}) - \Delta C_p \ln (T/T_{trs}) \quad (4)$$

where $\Delta H(T_{trs})$ is the molar transition enthalpy at T_{trs}, ΔC_p is the molar heat capacity change of unfolding, T is the temperature (K), and T_{trs} is the transition temperature.

The variance in $\Delta G_{N\rightarrow D}$ was calculated from (*5*):

$$\sigma^2_{\Delta G} = \left[\left(1 - \frac{T}{T_{trs}}\right)\sigma_{\Delta H}\right]^2 + \left[\left((T - T_{trs}) - T \ln \frac{T}{T_{trs}}\right)\sigma_{\Delta C_p}\right]^2 + \left[\left(\left(\frac{T}{T_{trs}} - 1\right)\Delta C_p + \frac{T}{T^2_{trs}}\Delta H_{trs}\right)\sigma_{\Delta T_m}\right]^2$$

RESULTS

Influence of the Intermolecular Disulfide Bridge on the Melting Temperature of EF-Ts. To investigate the effect of the intermolecular disulfide bridge in EF-Ts, the thermal denaturation of EF-Ts wild type (wt) in the absence or presence of 50 mM dithiothreitol and of EF-Ts(C190A) at low ionic strength and pH 7.0 was measured by DSC (Figure 2, boldface curves). Removal of the intersubunit disulfide bridge either by reduction with 50 mM dithiothreitol (*5*) or by site-directed mutagenesis (C190A, Figure 2B) shifted the thermal transition temperature of EF-Ts from 102.2 to 93 or 91 °C, respectively, with no effect on the calorimetric enthalpy (~400 kJ/mol). The virtually identical values of calorimetric enthalpies and transition temperatures of reduced EF-Ts(wt) and EF-Ts(C190A) indicate that the conformations of both proteins are very similar. The ratios of the van't Hoff and the calorimetric enthalpy are about 2 in the presence and absence of the disulfide bond, suggesting that the cooperative unit during the thermal transition is a dimer. This confirms previous results obtained by gel permeation chromatography at room temperature (*3*, *32*) that demonstrated that the intersubunit disulfide bond is not crucial for EF-Ts dimerization.

The heat-denatured samples were clear, and denaturation was apparently not accompanied by further heat-absorbing or heat-releasing processes, indicating that the unfolded polypeptide chains did not aggregate. After cooling of the heated samples, the area under the heat absorption peak of the second scan was reduced to 10% of that of the first scan (data not shown). This indicates a practically irreversible thermal denaturation of EF-Ts(wt) and its variant at low ionic strength and at pH 7.0. The nature of this irreversible process is unknown. However, if the irreversible step during thermal transition were connected to a significant change in enthalpy, an asymmetric DSC trace and/or a strong dependence of the transition temperature on scan rate and protein concentration would be expected (*33*, *34*). However, the transition temperature of the thermal denaturation of both proteins depends neither on protein concentration (10−90 μM) nor on scan rate (0.5−2.0 K/min) (data not shown), which indicates that an irreversible step occurs only above the transition temperature. It has been shown that in such a special case, despite irreversibility of thermal denaturation, the application of equilibrium thermodynamics to the transition does not lead to major errors (*33*). Indeed, the ratio of van't Hoff and calorimetric enthalpies is about 2, which is in accordance with the crystallographically observed dimer (*2*) and gel permeation chromatography experiments (*5*). Thus, an irreversible process connected with a significant enthalpy change does not take place, allowing the thermodynamic analysis of EF-Ts unfolding.

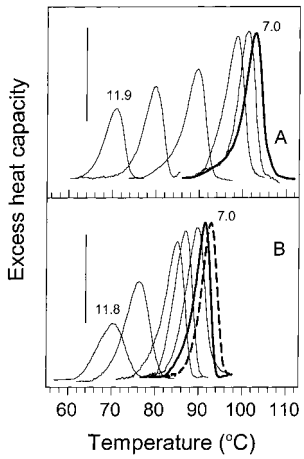

FIGURE 2: DSC measurements of EF-Ts in the presence and absence of an intermonomer disulfide bond. Corrected calorimetric recordings at different pHs of EF-Ts(wt) (A) shown from right to left were acquired at pH 7.0, 7.9, 9.0, 10.9, 11.6, and 11.9, and EF-Ts in the presence of 50 mM dithiothreitol (B) at pH 7.0 (dashed line), and EF-Ts(C190A) (B) at pH 7.0, 8.0, 9.1, 10.0, 11.0, and 11.8 (the extreme pH values are indicated). EF-Ts(wt) (A) and EF-Ts(C190A) (B) at pH 7.0 and EF-Ts in the presence of 50 mM dithiothreitol (B) are highlighted by thick lines for comparison. In all cases, the protein concentration was 22.2 μM in 10 mM sodium phosphate and 10 mM glycine buffers. The scan rate of heating was 1 K/min. Vertical lines designate a heat capacity of 1.0 mJ/K.

Effect of pH on the Stability of EF-Ts. EF-Ts is strongly charged, containing 68 negative, 66 positive charges, and 8 histidines per dimer and at least 34 ionic bonds per dimer at pH 7 (*3*). To estimate the contribution of electrostatic interactions between polypeptide chains to the stability of the homodimer, DSC measurements were performed in the range from pH 4.0 to pH 12.0. Corrected DSC traces of EF-Ts(wt) and EF-Ts(C190A) in the range of pH 7.0−12.0 are shown in Figure 2A and 2B, respectively. Despite irreversible thermal transitions, the DSC scans are symmetrical and without apparent distortions. The calculated isoelectric point of EF-Ts(wt) is 6.0. A shift of the pH below 7 will decrease the net charge of the protein surface and thus increase the likehood of nonspecific ionic interactions. Such nonspecific protein−protein interactions leading to aggregation are reflected by $\Delta H_{vH}/\Delta H_{cal} > 2$ below pH 7 (data not shown). As demonstrated by $\Delta H_{vH}/\Delta H_{cal}$ values close to 2 (Figure 3C) above pH 7, EF-Ts(wt) and also EF-Ts(C190A) remain in dimeric form under these conditions. Further thermodynamic analysis was therefore confined only to data obtained at pH >7.

Both transition temperature, T_{trs} (Figure 3A), and calorimetric enthalpy, ΔH_{cal} (Figure 3B), decrease with increasing pH. These pH-dependent profiles are in accordance with the isoelectric point of the protein, as an increasing pH causes a prevalence of negatively charged groups, that perturb the net of ionic interactions and lead to destabilization of the protein.

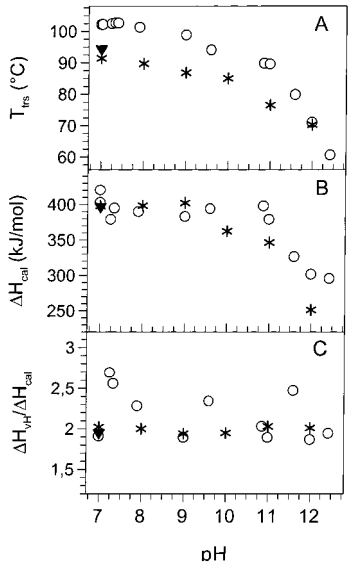

FIGURE 3: pH dependence of thermal transition temperatures of EF-Ts in the presence and absence of an intermonomer disulfide bond (A). Calorimetric enthalpies (B) and the ratio $\Delta H_{vH}/\Delta H_{cal}$ (C). EF-Ts(wt) (circles), EF-Ts(C190A) (stars), and EF-Ts(wt) in the presence of 50 mM dithiothreitol (triangles) at pH 7.0 are compared. Protein concentrations were 15.5−31.1 μM.

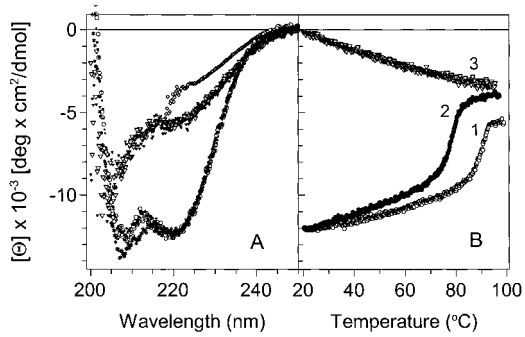

FIGURE 4: CD spectra of EF-Ts in the presence and absence of an intermonomer disulfide bond. (A) EF-Ts(wt) (open circles), EF-Ts(C190A) (closed circles) at 20 °C; EF-Ts(wt) (open triangles), EF-Ts(C190A) (closed triangles) at 105 °C; after recooling of EF-Ts(wt) from 105 to 20 °C (stars) in 10 mM phosphate buffer, pH 7.0, and Ts(wt) in 6.0 M guanidine hydrochloride, 10 mM sodium phosphate buffer, pH 7.0 at 105 °C (diamonds). The protein concentration was 2.5 μM. (B) Temperature denaturation of EF-Ts(C190A) without (1) and in the presence of 0.70 M (2) and 6.0 M (3) guanidine hydrochloride observed at 222 nm in 10 mM phosphate buffer, pH 7.0. Protein concentration was 2.5 μM. The ellipticity is reported as the mean residue ellipticity.

Structure of the Thermally Unfolded EF-Ts. The thermodynamic parameters of the thermal unfolding of EF-Ts(wt) and EF-Ts(C190A) can be compared only under the premise that the native and thermal unfolded states of both proteins are very similar. Therefore, the CD spectra of EF-Ts(wt) and EF-Ts(C190A) in native (20 °C) and denatured (105 °C) states were compared (Figure 4A). The shape and mean molar ellipticities of the CD spectra at 20 °C of both proteins are almost identical. This indicates that EF-Ts(C190A) retains the same secondary structure as EF-Ts(wt) under these conditions. Similar results were obtained with both proteins over a pH range from 4.0 to 12.0; i.e., the secondary structures of the both proteins remain unperturbed within this pH range. The comparison of CD spectra of EF-Ts at 105 °C in the presence and in the absence of 6.0 M guanidine hydrochloride revealed that EF-Ts retained part of its secondary structure even at harsh conditions beyond the boiling point of water (Figure 4A). Cooling of the heated sample leads to a nearly complete recovery of the secondary structure, whereas the restored tertiary structure differs from that of the native state. This is based on the DSC measurements that showed that after the first heating and cooling, reheating induces a noncooperative thermal denaturation of the sample. The preserved secondary structure and perturbed tertiary structure most likely can be described by a molten globule-like state of the recooled EF-Ts after thermal transition.

Further evidence for the persistent secondary structure was obtained from thermal transition experiments of EF-Ts(C190A) monitored by CD at 222 nm in the presence of guanidine hydrochloride. Figure 4B demonstrates that residual secondary structure, reflected by the negative ellipticity at 95 °C in the absence of denaturants (trace 1), already unfolds in the presence of relatively small concentrations of guanidine hydrochloride (trace 2). This residual ellipticity is identical with that of EF-Ts(C190A) in the presence of 6 M guanidine hydrochloride at 95 °C (trace 3). The persistent secondary structure cannot be destroyed by high ionic strength (2 M NaCl) (data not shown), suggesting that it is stabilized predominantly by hydrophobic and not by ionic interactions.

Effect of Chaotropic Salts on the Thermal Stability of EF-Ts. CD measurements indicate a nearly complete reversibility of secondary structure unfolding of EF-Ts in thermal denaturation/renaturation experiments (Figure 4A). On the other hand, the tertiary structure of EF-Ts(wt) and EF-Ts(C190A) could not be restored by cooling a denatured sample as judged by DSC. This prompted us to find suitable conditions under which a correctly folded protein is formed. Incorrect interactions during refolding can be avoided by the optimal concentration of denaturants such as urea, or chaotropic salts such as guanidine hydrochloride or $NaClO_4$. With EF-Ts(C190A), a full reversibility of the thermal transition was observed in the presence of 2.5 M $NaClO_4$ (data not shown). According to the Hofmeister anion series, the chaotropic perchlorate anion "salts-in" the peptide group, and consequently interacts more strongly with the unfolded form of a protein than with its native form (*35*).

Thermodynamic parameters determined from the analysis of DSC thermograms of EF-Ts(wt) and its variant C190A at different concentrations of $NaClO_4$ are shown in Figure 5. The transition temperatures of both EF-Ts(wt) and EF-Ts(C190A) decrease linearly with increasing salt concentrations (Figure 5A). The replacement of cysteine 190 for alanine increases the sensitivity of the calorimetric enthalpy to $NaClO_4$, as reflected by its steeper linear decrease in the case of EF-Ts(C190A) in comparison to that of EF-Ts(wt) (Figure 5B). The observed difference in sensitivity of EF-Ts(wt) and its variant C190A toward the denaturing effect of $NaClO_4$ seems to indicates that the intermolecular disulfide bond decreases the penetration of the salt into the dimer interface. The $\Delta H_{vH}/\Delta H_{cal}$ values (Figure 5C) suggest that the cooperative unit of EF-Ts(C190A) is a dimer even at high concentrations of $NaClO_4$.

In Figure 5D the reversibilities of the thermal denaturation of EF-Ts(wt), EF-Ts(C190A), and EF-Ts(wt) in the presence of 50 mM dithiothreitol at different $NaClO_4$ concentrations

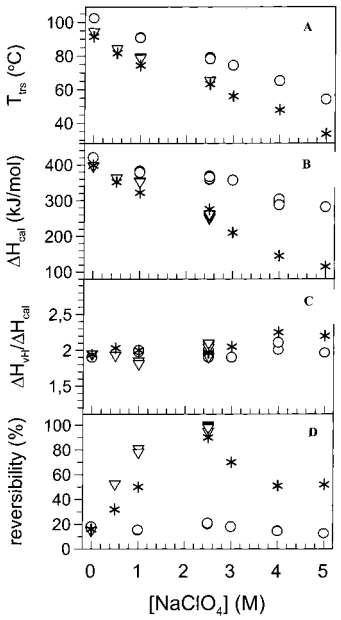

FIGURE 5: Effect of $NaClO_4$ concentration on the calorimetric enthalpy, ΔH_{cal} (A), the temperature of the thermal transition, T_{trs} (B), the ratio $\Delta H_{vH}/\Delta H_{cal}$ (C), and the reversibility of the thermal transitions (D) of EF-Ts(wt) (circles), EF-Ts(C190A) (stars), and EF-Ts(wt) in the presence of 50 mM dithiothreitol (triangles) in 10 mM phosphate buffer, pH 7.0. Protein concentrations were 15.5−31.1 μM.

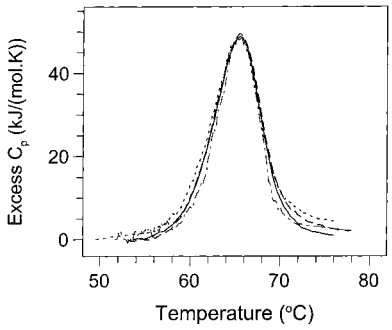

FIGURE 6: Temperature dependence of the excess heat molar capacity of EF-Ts(wt) at different protein concentrations: 9.8 (− · −), 20.0 (---), 29.8 (− −), and 57.3 (—) μM in the presence of 50 mM dithiothreitol in 10 mM sodium phosphate buffer, pH 7.0, and 2.5 M $NaClO_4$.

are compared. In the absence of the disulfide bridge, the reversibility is significantly higher with an optimum at 2.5 M $NaClO_4$. The high reversibility of the thermal transition of EF-Ts(C190A) in the absence of the reducing agent is surprising, since EF-Ts possesses an additional cysteine at position 78 which could interfere with refolding. Apparently, even at high temperatures this residue is hindered from disulfide bond formation by residual secondary structure.

In Figure 6 the calorimetric traces, expressed in molar calorimetric enthalpy, of EF-Ts(wt) in the presence of 50 mM dithiothreitol at 2.5 M $NaClO_4$ are shown. Enthalpy and transition temperature do not depend on protein concentration in the range from 0.22 to 1.29 mg/mL (10−60 μM) under these conditions. Accordingly, transition temperatures and van't Hoff enthalpies are 101.5 °C and 818.6 kJ/mol per dimer for EF-Ts(wt) and 91.1 °C and 683.8 kJ/mol per dimer for EF-Ts(C190A), respectively. Thus, the values obtained by CD at a protein concentration of 0.056 mg/mL correspond to the values determined calorimetrically. This further

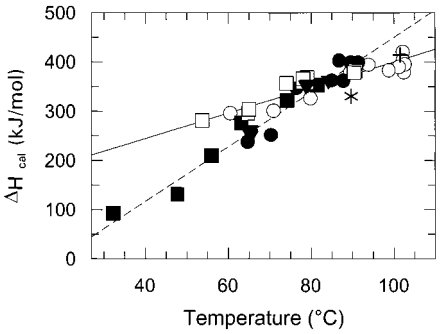

FIGURE 7: Enthalpies of thermal transition of EF-Ts(wt) (empty symbols) and EF-Ts(C190A) (solid symbols) measured at various pHs and $NaClO_4$ concentrations, respectively, and EF-Ts(wt) in the presence of 50 mM dithiothreitol (triangles) at different $NaClO_4$ concentrations plotted against transition temperatures. Cross and star symbols depict $\Delta H_{vH}/2$ values, i.e., ΔH_{vH} per monomer, obtained from CD measurements of EF-Ts(wt) and EF-Ts(C190A) variant, respectively, at pH 7.0 in 10 mM sodium phosphate buffer. From the slopes of the linear regressions, $\Delta C_p = 2.59 \pm 0.24$ kJ/(mol·K) per monomer (correlation coefficient $R = 0.923$) for EF-Ts(wt) and $\Delta C_p = 5.55 \pm 0.34$ kJ/(mol·K) per monomer ($R = 0.965$) for EF-Ts(C190A) or reduced EF-Ts(wt) were calculated.

underlines the notion that the dimer is the cooperative unit of the thermal transition.

Estimation of ΔC_p and ΔG of the Thermal Unfolding of EF-Ts. Enthalpy transitions, ΔH_{cal}, and dependencies on transition temperatures, T_{trs}, obtained at different pHs and $NaClO_4$ concentrations, for both wt and C190A variant are shown in Figure 7. Heat capacity changes, ΔC_p, upon unfolding for both proteins were calculated from the slopes of the linear regressions. The ΔC_p values were 2.59 ± 0.24 kJ/(mol·K) per monomer EF-Ts(wt) and 5.55 ± 0.34 kJ/(mol·K) per monomer for EF-Ts(C190A) and reduced EF-Ts(wt), respectively. As expected, ΔC_p for the dimer containing the disulfide bridge is smaller than ΔC_p for the dimer without the disulfide bridge. This reflects an increase in the accessible surface area of the dimeric EF-Ts in the absence of the disulfide bond.

The results of this investigation demonstrate that the thermal unfolding of EF-Ts(wt) and the EF-Ts(C190A) proceeds as a cooperative two-state transition in the range from 20 to 105 °C. Both the native and the unfolded states of the proteins are dimers. The obtained values of ΔC_p, T_{trs}, and ΔH_{cal} enabled us to calculate the stabilization effect of the disulfide bridge in the dimer of EF-Ts. The contribution of the disulfide bridge to the stability of EF-Ts, at 72.5 °C, is $\Delta\Delta G_{(S-S,SH\ HS)} = 10.5$ kJ/mol per monomer (Figure 8A). The relatively low ΔC_p of EF-Ts(wt) flattens the dependence of the free energy on temperature. Therefore, the maximum stability of EF-Ts(wt) is at lower temperatures as compared to EF-Ts(C190A). EF-Ts(wt) with the disulfide bridge is more stable than the variant C190A at all temperatures (Figure 8A).

DISCUSSION

Effect of the Intermonomer Disulfide Bond on the Reversibility of the Thermal Transition. Proteins from thermophiles are usually extremely stable and have high transition temperatures, frequently above the boiling point of water. Often, their thermodynamic characterization is impeded by irreversible side reactions during the thermal analysis, e.g., irrevers-

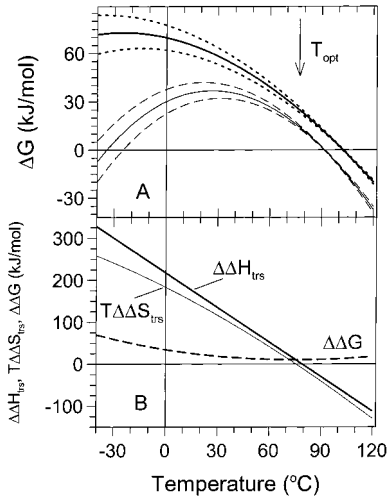

FIGURE 8: (A) Stability profiles of EF-Ts(wt) (upper curve) and EF-Ts(C190A) (lower curve) at pH 7.0 calculated from T_{trs}, ΔH_{cal}, and ΔC_p 102.2 °C, 402.2 kJ/mol, and 2.59 kJ mol^{-1} K^{-1} and 91.7 °C, 398.8 kJ/mol, and 5.55 kJ mol^{-1} K^{-1}, respectively, as a function of temperature calculated according to eq 4. Ranges of experimental error are $T_{trs} \pm 0.3$ K, $\Delta H_{cal} \pm 10\%$, and $\Delta C_p \pm 10\%$. The error limits for ΔG_{unf} at pH 7.0, calculated according to eq 5, are indicated by dashed and dotted lines for EF-Ts(wt) and EF-Ts(C190A), respectively. The optimal growth temperature of *T. thermophilus* is indicated by the arrow. (B) Temperature dependence of the calculated differences of transition enthalpies, ΔH_{trs}(EF-Ts(wt)) − ΔH_{trs}(EF-Ts(C190A)) = $\Delta\Delta H_{trs}$, entropy changes upon unfolding, ΔS_{trs}(EF-Ts(wt)) − ΔS_{trs}(EF-Ts(C190A)) = $\Delta\Delta S_{trs}$, and free energies, ΔG(EF-Ts(wt)) − ΔG(EF-Ts(C190A)) = $\Delta\Delta G$, of EF-Ts(wt) and EF-Ts(C190A). Values of 375.35 K, 402.2 kJ/mol, 2.59 kJ/(mol·K) and 364.85 K, 398.8 kJ/mol, 5.55 kJ/(mol·K) for T_{trs}, ΔH_{trs}, and ΔC_p of EF-Ts(wt) and EF-Ts(C190A), respectively, obtained by DSC measurements in 10 mM sodium phosphate buffer (pH 7.0) were used. The ranges of the experimental error are $T_{trs} \pm 0.3$ K, $\Delta H_{cal} \pm 10\%$, and $\Delta C_p \pm 10\%$, respectively.

ible chemical modification or aggregation (*36*). The thermal transition of EF-Ts from *T. thermophilus* is irreversible at low ionic strength. Nevertheless, it can be analyzed by equilibrium thermodynamics because: (i) precipitation or aggregation did not occur during DSC measurements; (ii) as demonstrated by CD spectroscopy, cooling of the heated sample resulted in nearly complete recovery of the secondary structure of both oxidized and reduced forms of EF-Ts over a broad pH range; and (iii) the ratio $\Delta H_{vH}/\Delta H_{cal}$ of 2 is in agreement with the crystal structure of EF-Ts(wt) (*2*, *3*). This points to a dimeric cooperative unit during the thermal denaturation, and aggregation of EF-Ts would result in $\Delta H_{vH}/\Delta H_{cal} > 2$.

Recently, it was observed that the presence of a chaotropic agent significantly increases the reversibility of the thermal transition of the homodimeric spherulin 3a from *Physarum polycephalum* (*37*). In a similar manner, $NaClO_4$ improves the reversibility of the thermal transition of EF-Ts provided that the intersubunit disulfide bridge is absent. The complete recovery of EF-Ts(wt) tertiary structure in the presence of 2.5 M $NaClO_4$ and 50 mM dithiothreitol indicates that irreversible chemical modification of cysteine residues does not take place during thermal denaturation. Thus, the intermonomer disulfide bridge probably decreases the flexibility of the hydrophobic dimer interface and prevents the correct folding of EF-Ts(wt) (Figure 5D).

Comparison of the Dimer Interface in the Absence and Presence of the Disulfide Bond. The extent of exposure of buried surface area to solvent upon unfolding is reflected by two thermodynamic parameters, the partial molar heat capacity ΔC_p and the denaturant *m* value, which are generally dominated by the positive contribution of solvating nonpolar surfaces (*38*).

Thermal unfolding of dimeric proteins may be generally described by the scheme:

$$N_2 \rightleftharpoons I_2 \rightleftharpoons 2U\ (U_2)$$

where N_2 is the native dimer, I_2 is the partially unfolded dimeric intermediate, U is the completely unfolded monomer (for noncovalently connected dimers), and U_2 is the completely unfolded dimer (for covalently linked dimers). The ΔC_p values for two-state $N_2 \rightleftharpoons 2U$ processes are in the same range (*23*, *39*, *40*) as those for monomeric proteins (*41*). A three-state thermal unfolding was described for the dimeric *E. coli Trp* repressor (*40*). Despite an apparently complete exposure of the aromatic side chains, the thermal transition $N_2 \rightleftharpoons I_2$ of this protein was characterized by a small ΔC_p. This observation is similar to the very low ΔC_p obtained for the thermal transition of $(EF\text{-}Ts)_2$. In fact, the ΔC_p values obtained for EF-Ts(wt) and EF-Ts(C190A), of 2.59 (±0.24) kJ/(mol·K) and 5.55 (±0.34) kJ/(mol·K) per monomer, respectively, are significantly lower than the values calculated from the difference in accessible surface area (ΔASA) of the protein in its native and denatured states (*38*). In this calculation, the linear dependence of ΔASA on the number of residues ($N_{res} = 196$), $\Delta ASA \sim -907 + 93N_{res}$, is used to determine ΔC_p. ΔC_p should be the same for the oxidized and reduced forms of EF-Ts, $\Delta C_p \sim -251 + 0.19\Delta ASA = 12.73$ kJ/(mol·K) per monomer. Vice versa, from obtained ΔC_p values, it is possible to calculate the number of residues taking part in thermal unfolding. Here, we obtain 59 and 99 residues for EF-Ts(wt) and EF-Ts(C190A), respectively. These numbers are in conflict with the total number of amino acid residues in EF-Ts and indicate different exposure of the buried surface area of EF-Ts(wt) and EF-Ts(C190A) upon thermal denaturation. The persistent secondary structure of EF-Ts(wt) and EF-Ts(C190A) even above transition temperatures (Figure 4) as well as the independence of their thermal transitions on protein concentration (Figure 6) strongly suggests the existence of dimeric intermediates under these conditions. Thus, EF-Ts remains in the intermediate dimeric state, and the measured thermal transitions of EF-Ts can be described by the scheme:

$$N_2 \rightleftharpoons I_2$$

However, even if the 2156 Å^2 of ΔASA of the buried interface in the EF-Ts dimer (*3*) is not considered, the calculated ΔC_p is still significantly higher than the experimentally determined value (data not shown). Therefore, additional factors must influence the ΔC_p value.

First, the contribution of the N-terminal domain of EF-Ts to ΔC_p is probably minimal. This domain is disordered in the crystal structure of EF-Ts (*3*), and its removal does not affect the stability of the protein (*42*). The reported ΔC_p value of a 50-residue-long helical peptide, which is close to 0 (*43*), suggests that the contribution of a similar α-helical N-domain of EF-Ts to ΔC_p is also minimal. Thus, a major contribution to ΔC_p of EF-Ts originates from the structure of the

C-domain. Second, the persistent secondary structure of both the oxidized and reduced forms of EF-Ts observed at 105 °C probably contains antiparallel β-strands (Figure 1). Nevertheless, a minimum at 222 nm in the CD spectra (Figure 4) indicates a small contribution of α-helix (*44*). Such a stable core of EF-Ts(wt) is in agreement with the presence of both intermolecular and intramolecular interactions that stabilize the entire dimeric region (Figure 1).

If both the amino acid residues of the N-domain and the residues buried in the dimer interface are neglected, the calculated ΔC_p is 7.31 kJ/(mol·K) per monomer. However, this value is still higher than the experimentally determined values of ΔC_p of the oxidized and reduced forms of EF-Ts. The small ΔC_p therefore may reflect the differences in the dynamics of the persistent secondary structures in oxidized and reduced forms of EF-Ts above transition temperatures. The localization of the disulfide bond close to the carboxyl ends of both polypeptides probably rigidifies not only the dimeric interface but, also through long-distance interactions, also the conformation of the entire $(EF\text{-}Ts)_2$. Moreover, it can be assumed that the unfolded N-domain, which is connected to the edge of the β-sheet of the dimer interface by a polypeptide hinge, destabilizes this region at high temperatures (*42*). This may contribute significantly to the increased ΔC_p of EF-Ts(C190A) relative to that of EF-Ts(wt).

Temperature Dependence of Thermodynamic Parameters. Dependencies of ΔH_{trs}, ΔS_{trs}, and ΔG (Figure 8A) on temperature can be calculated by utilizing ΔC_p values and the thermodynamic parameters of thermal transitions of oxidized and reduced EF-Ts forms. Comparison of these parameters allowed us to assess the effect of temperature and the role of the disulfide bond on the stability of $(EF\text{-}Ts)_2$. From this thermodynamic analysis, it follows that: (i) the intermonomer disulfide bond stabilizes the EF-Ts dimer over a wide temperature range; (ii) the difference of ΔG(EF-Ts(wt)) − ΔG(EF-Ts(C190A)) has a minimum at the optimal growth temperature of *T. thermophilus* (70−75 °C) (Figure 8B); (iii) the gain in stability due to the disulfide bond is caused by an enthalpic factor at temperatures below 77 °C and by an entropic factor at higher temperatures (Figure 8B).

Thus, the nature of stabilization of $(EF\text{-}Ts)_2$ by the disulfide bond is complex. In accordance with Doig and Williams (1991) (*18*), we propose that a diminished exposure of hydrophobic residues due to the intermonomer disulfide bond results in a decreased ordering of solvents (hydrophobic effect), as manifested by a small ΔC_p and positive $\Delta\Delta S_{trs}$ below 77 °C. In terms of enthalpy, the disulfide cross-link destabilizes the unfolded state, since the hydrogen bond network is energetically less favorable in an unfolded state, which is constrained by the cross-link compared to an unconstrained random coil (*18*). However, in the case of EF-Ts(wt) and EF-Ts(C190A), the thermally denatured states are far from unconstrained random coils. Thus, a positive $\Delta\Delta H_{trs}$ at lower temperatures is probably induced by the rigidity of the dimer interface cross-linked by the disulfide bond which strengthens intermonomer interactions in the interface. The hydrophobic effect increases with temperature (*41*), as reflected by the decreasing ellipticity at 222 nm of EF-Ts (Figure 4B, curve 3). The decreased difference in flexibility of the oxidized and reduced forms of EF-Ts at high temperature is reflected by a decrease in $\Delta\Delta H_{trs}$ (Figure 8B). The value of this parameter became negative above 79 °C, i.e., when the effect of the cross-link on the denatured state is overcompensated, the hydrophobic effect in the dimer interface (*18*). Therefore, the difference of ΔS(EF-Ts(wt)) − ΔS(EF-Ts(C190A)) is negative at temperatures above 75 °C, where the effect of the disulfide bridge on the conformational entropy of the polypeptide chain of EF-Ts(wt) is outweighed by an increased entropy of the more flexible denatured state of EF-Ts(C190A).

Strategies Implied in Stabilization of the Dimer Interface. In addition to hydrophobic interactions, there are several electrostatic interactions of amino acid side chains, located at the edge of the interface (Figure 1). Either these are intramolecular, as in Arg191/Glu193, or they create a net of intra- and intermolecular interactions, as may be seen between the Glu75 and Arg188 of one subunit and the carboxy terminus of Ala196 of the second subunit. Importantly, these interactions are doubled due to the 2-fold symmetry of the dimer.

The results of several recent investigations indicate that electrostatic interactions contribute significantly to the stability of thermophilic and hyperthermophilic proteins (*45*, *46*). In hyperthermophilic proteins, the electrostatic interactions are enhanced by optimal placement of the charged amino acid residues within the structure of the protein. Further contributions to protein stability were ascribed to interactions that reduce the entropy of the unfolded state (*47*). Our work demonstrates that both of these principles, optimal localization of ionic interactions on the symmetrical dimer interface and the covalent link between domains, contribute to the stabilization of EF-Ts.

Recently, it was demonstrated that electrostatic interactions between amino acid residues of N- and C-termini are crucial for thermostability of the monomeric cold shock protein from *Bacillus caldolyticus* (*48*). In EF-Ts, such interactions involve two polypeptide chains. The 2-fold symmetry of the EF-Ts dimer suggests a strategy in the evolution of thermophiles, where one point mutation exercises its stabilization effect twice. It is interesting to note that high concentrations of neither urea (9 M), as a nonionic denaturant, nor NaCl (2 M), as a purely ionic agent, were capable of perturbing the secondary structure and the stability of EF-Ts(C190A) (data not shown). In contrast, the presence of ionic chaotropic agents such as perchlorate or guanidine hydrochloride affects the stability and structure of EF-Ts even at low concentrations (Figure 4). Thus, a synergistic effect of a number of hydrophobic and electrostatic interactions in the dimer interface of $(EF\text{-}Ts)_2$ may explain the observed extreme stability.

Biological Implications of Extreme Stability of Dimeric EF-Ts. The structure of the EF-Ts dimer from the extreme thermophile *T. thermophilus* is similar to that of the EF-Ts monomer from the mesophile *E. coli* (*1*, *2*). A dimeric structure was also observed in EF-1β from the thermoacidophilic archaeon *Sulfolobus solfataricus* (*49*). Here, we demonstrate that dimer formation can efficiently contribute to the overall thermal stability of the protein and that the symmetric arrangement of the dimer interfaces may be an important principle in the evolution of proteins in thermophiles. Thus, the compact interface of dimeric EF-Ts from *T. thermophilus* may reflect the evolution toward achieving a high degree of stability at the physiological temperatures

of thermophiles with relatively short polypeptide chains. On the other hand, the stability of an enzyme far beyond the growth temperature of the organism may result in poor catalytic efficiency as flexibility is required for activity (*50*). However, this may not be a disadvantage for proteins with a solely mechanical nature of action, e.g., cytochrome *c* (*51*), or ferredoxin (*52*), or EF-Ts. EF-Ts forms a complex with EF-Tu·GDP and induces a conformational change in EF-Tu leading to dissociation of the nucleotide (*1*, *2*). Since the flexibility of nucleotide-free EF-Tu is considerably higher than that of nucleotide-bound forms, EF-Tu·GDP and EF-Tu·GTP, it is reasonable to expect that in a stable $(EF\text{-}Ts)_2$·EF-Tu complex EF-Tu is stabilized by EF-Ts in a strained conformation that is optimal for reaction with GTP.

ACKNOWLEDGMENT

We thank Dr. Alexandra Wolfrum for advice during protein purifications, Stephan Brock, Drs. Markus Rudolph, and Dagmar Klostermeier for helpful discussions, and Norbert Grillenbeck for excellent technical assistance.

REFERENCES

1. Kawashima, T., Berthet-Colominas, C., Wulff, M., Cusack, S., and Leberman, R. (1996) *Nature 379*, 511−518.
2. Wang, Y., Jiang, Y., Meyering-Voss, M., Sprinzl, M., and Sigler, P. B. (1997) *Nat. Struct. Biol. 4*, 650−656.
3. Jiang, Y., Nock, S., Nesper, M., Sprinzl, M., and Sigler, P. B. (1996) *Biochemistry 35*, 10269−10278.
4. Nesper, M., Nock, S., Sedlak, E., Antalik, M., Podhradsky, D., and Sprinzl, M. (1998) *Eur. J. Biochem. 255*, 81−86.
5. Blank, J., Nock, S., Kreutzer, R., and Sprinzl, M. (1996) *Eur. J. Biochem. 236*, 222−227.
6. Zhang, Y., Tao, J., Zhou, M., Meng, Q., Zhang, L., Shen, L., Klein, R., and Miller, D. L. (1997) *Arch. Biochem. Biophys. 344*, 43−52.
7. Volkin, D. B., and Klibanov, A. M. (1987) *J. Biol. Chem. 262*, 2945−2950.
8. Gromiha, M. M., Oobatake, M., and Sarai, A. (1999) *Biophys. Chem. 82*, 51−67.
9. Jones, S., and Thornton, J. M. (1995) *Prog. Biophys. Mol. Biol. 63*, 31−65.
10. DeDecker, B. S., O'Brien, R., Fleming, P. J., Geiger, J. H., Jackson, S. P., and Sigler, P. B. (1996) *J. Mol. Biol. 264*, 1072−1084.
11. Maes, D., Zeelen, J. P., Thanki, N., Beaucamp, N., Alvarez, M., Thi, M. H., Backmann, J., Martial, J. A., Wyns, L., Jaenicke, R., and Wierenga, R. K. (1999) *Proteins: Struct., Funct., Genet. 37*, 441−453.
12. Hopfner, K. P., Eichinger, A., Engh, R. A., Laue, F., Ankenbauer, W., Huber, R., and Angerer, B. (1999) *Proc. Natl. Acad. Sci. U.S.A. 96*, 3600−3605.
13. Singleton, M., Isupov, M., and Littlechild, J. (1999) *Struct. Fold. Des. 7*, 237−244.
14. Toth, E. A., Worby, C., Dixon, J. E., Goedken, E. R., Marqusee, S., and Yeates, T. O. (2000) *J. Mol. Biol. 301*, 433−450.
15. Matsumura, M., and Matthews, B. W. (1991) *Methods Enzymol. 202*, 336−356.
16. Creighton, T. E. (1988) *Bioessays 8*, 57−63.
17. Cooper, A., Eyles, S. J., Radford, S. E., and Dobson, C. M. (1992) *J. Mol. Biol. 225*, 939−943.
18. Doig, A. J., and Williams, D. H. (1991) *J. Mol. Biol. 217*, 389−398.
19. Kirino, H., Aoki, M., Aoshima, M., Hayashi, Y., Ohba, M., Yamagishi, A., Wakagi, T., and Oshima, T. (1994) *Eur. J. Biochem. 220*, 275−281.
20. Rietveld, A. W., and Ferreira, S. T. (1998) *Biochemistry 37*, 933−937.
21. Villeret, V., Clantin, B., Tricot, C., Legrain, C., Roovers, M., Stalon, V., Glansdorff, N., and Van Beeumen, J. (1998) *Proc. Natl. Acad. Sci. U.S.A. 95*, 2801−2806.
22. Thoma, R., Hennig, M., Sterner, R., and Kirschner, K. (2000) *Struct. Fold. Des. 8*, 265−276.
23. Griko, Y. V., Rogov, V. V., and Privalov, P. L. (1992) *Biochemistry 31*, 12701−12705.
24. Liang, H., Sandberg, W. S., and Terwilliger, T. C. (1993) *Proc. Natl. Acad. Sci. U.S.A. 90*, 7010−7014.
25. Gokhale, R. S., Agarwalla, S., Francis, V. S., Santi, D. V., and Balaram, P. (1994) *J. Mol. Biol. 235*, 89−94.
26. Tamura, A., Kojima, S., Miura, K., and Sturtevant, J. M. (1994) *Biochemistry 33*, 14512−14520.
27. Byrne, M. P., and Stites, W. E. (1995) *Protein Sci. 4*, 2545−2558.
28. Sanchez-Ruiz, J. M., Lopez-Lacomba, J. L., Cortijo, M., and Mateo, P. L. (1988) *Biochemistry 27*, 1648−1652.
29. Hu, C. Q., and Sturtevant, J. M. (1987) *Biochemistry 26*, 178−182.
30. Sturtevant, J. M. (1987) *Annu. Rev. Phys. Chem. 38*, 463−488.
31. Pace, C. N., Vajdos, F., Fee, L., Grimsley, G., and Gray, T. (1995) *Protein Sci. 4*, 2411−2423.
32. Arai, K., Ota, Y., Arai, N., Nakamura, S., Henneke, C., Oshima, T., and Kaziro, Y. (1978) *Eur. J. Biochem. 92*, 509−519.
33. Sanchez-Ruiz, J. M. (1992) *Biophys. J. 61*, 921−935.
34. Lyubarev, A. E., and Kurganov, B. I. (1999) *Biochemistry (Moscow) 64*, 832−838.
35. Baldwin, R. L. (1996) *Biophys. J. 71*, 2056−2063.
36. Ahern, T. J., and Klibanov, A. M. (1985) *Science 228*, 1280−1284.
37. Kretschmar, M., and Jaenicke, R. (1999) *J. Mol. Biol. 291*, 1147−1153.
38. Myers, J. K., Pace, C. N., and Scholtz, J. M. (1995) *Protein Sci. 4*, 2138−2148.
39. Steif, C., Weber, P., Hinz, H. J., Flossdorf, J., Cesareni, G., and Kokkinidis, M. (1993) *Biochemistry 32*, 3867−3876.
40. Gloss, L. M., and Matthews, C. R. (1997) *Biochemistry 36*, 5612−5623.
41. Privalov, P. L., and Gill, S. J. (1988) *Adv. Protein Chem. 39*, 191−214.
42. Valusova, E., Sedlak, E., Antalik, M., Nock, S., and Sprinzl, M. (2001) *Biochim. Biophys. Acta 1547*, 117−126.
43. Scholtz, J. M., Marqusee, S., Baldwin, R. L., York, E. J., Stewart, J. M., Santoro, M., and Bolen, D. W. (1991) *Proc. Natl. Acad. Sci. U.S.A. 88*, 2854−2858.
44. Johnson, W. C. Jr. (1990) *Proteins: Struct., Funct., Genet. 7*, 205−214.
45. Vetriani, C., Maeder, D. L., Tolliday, N., Yip, K. S., Stillman, T. J., Britton, K. L., Rice, D. W., Klump, H. H., and Robb, F. T. (1998) *Proc. Natl. Acad. Sci. U.S.A. 95*, 12300−12305.
46. Xiao, L., and Honig, B. (1999) *J. Mol. Biol. 289*, 1435−1444.
47. Van den Burg, B., Vriend, G., Veltman, O. R., Venema, G., and Eijsink, V. G. (1998) *Proc. Natl. Acad. Sci. U.S.A. 95*, 2056−2060.
48. Perl, D., Mueller, U., Heinemann, U., and Schmid, F. X. (2000) *Nat. Struct. Biol. 7*, 380−383.
49. Raimo, G., Masullo, M., Savino, G., Scarano, G., Ianniciello, G., Parente, A., and Bocchini, V. (1996) *Biochim. Biophys. Acta 1293*, 106−112.
50. Rehaber, V., and Jaenicke, R. (1992) *J. Biol. Chem. 267*, 10999−11006.
51. Florens, L., Bianco, P., Haladjian, J., Bruschi, M., Protasevich, I., and Makarov, A. (1995) *FEBS Lett. 373*, 280−284.
52. Pfeil, W., Gesierich, U., Kleemann, G. R., and Sterner, R. (1997) *J. Mol. Biol. 272*, 591−596.

BI010274E